DUAL-STAGE ALGORITHM TO IDENTIFY CHANNELS WITH POOR ELECTRODE-TO-NEURON INTERFACE IN COCHLEAR IMPLANT USERS

Stefano Cosentino[1], Lindsay DeVries[2], Rachel Scheperle[3], Julie Bierer[2], and Robert Carlyon[1]

[1] MRC Cognition and Brain Sciences Unit, Cambridge, UK
[2] University of Washington, Seattle, USA
[3] University of Iowa, Iowa, USA

ABSTRACT

Users of cochlear implants rely on a number of electrodes to perceive acoustic information. The extent to which their hearing is restored depends on a number of factors including the electrode-to-neuron interface. We describe an approach to detect instances of poor-performing channels based on physiological data known as electrically evoked compound action potentials (ECAPs). The proposed approach - termed Panoramic ECAP ("PECAP") - combines nonlinear optimization stages with different constraints to recover neural activation patterns for all electrodes. Data were obtained from nine cochlear implant subjects and used to run the PECAP tool to identify possible instances of poor-performing channels. Data from one subject revealed a shifted peak ("dead region").

Index Terms — Biomedical signals, Cochlear Implant, ECAP, Electrode-to-Neuron interface, Diagnostic tool.

1. INTRODUCTION

Cochlear implants (CI) are hearing restoration devices that operate by converting acoustic sounds into electrical pulses delivered to a discrete number of electrodes, between 12 and 22 [1]. Different frequency-to-electrode channels may contribute differently to the outcome of the device depending on a number of factors, such as: the exact position of the electrode array inside the cochlea, the surgical procedure adopted, or the neural survival around the electrodes [2, 3]. Being able to detect instances of poor-performing channels is of clinical interest, as it can inform subject-specific programming options [4]. In this study we revised an algorithm – termed PECAP – that was recently described in [5], and further validated the approach using physiological data from nine cochlear implant users [6].

The physiological measurements consisted of evoked compound action potentials, ECAPs [7], which were measured by DeVries *et al.* [6] using a forward-masking procedure (e.g., as described in [8]). According to this procedure, a compound neural response is obtained stimulating two electrodes, one acting as masker and the other as probe. The amplitude of the ECAP waveform reflects the *joint excitation pattern* of both the probe and the masker neural activation patterns (AP, also known as "excitation pattern"). Hence, for a given combination of masker and probe electrodes p and m, the measured ECAP amplitude is expected to be:

$$M_{p,m} = \sum_k A_p(k) \cdot A_m(k) \quad (1)$$

where $A_i(k)$ is the neural AP produced by electrode i stimulated at most comfortable level (MCL) as function of place k along the cochlea. Consistent with the above notation, the matrix containing the ECAP amplitudes for all combinations of p and m will be:

$$\boldsymbol{M} = \boldsymbol{A} \cdot \boldsymbol{A}^T \quad (2)$$

As only matrix $\boldsymbol{M}$ is observable, it is necessary to solve the inverse problem to obtain the activation pattern for all electrodes ($\boldsymbol{A}$). Unfortunately the solution is not unique, and there are an infinite number of solutions $\boldsymbol{A}$ that can solve Eq. 2. Our approach, first described in [5], is to apply a multi-stage nonlinear algorithm where different constraints are used to limit the number of solutions $\boldsymbol{A}$. In particular, STAGE II is aimed at the detection of possible *unwanted exceptions* in the electrode-to-neuron interface. Examples of such exceptions are dead regions or cross-turn stimulation, which produce activation patterns that, respectively, have peaks shifted away from the stimulating electrode or are bimodal [9]. Both exceptions will likely affect the shape of the neural activation patterns, but their effects may not be visible from the measured ECAP (i.e., $\boldsymbol{M}$) where the effect of probe and masker is mixed; thus we advocate our PECAP approach as a more accurate method to infer information about the neural AP from ECAP measurements than using simple ECAP masking patterns (i.e., $M_{p,m}$).

In this study, the PECAP algorithm was further refined in the normalization stage. The algorithm was run on a dataset of nine subjects to detect instances of possible exceptions and to predict neural activation patterns for all electrodes.

The remainder of this paper is organized as follows. The PECAP algorithm and the proposed modification are described in Section 2 and 3. Section 4 describes the the experimental setup, while section 5 reports and discusses the results. Conclusion follows in Section 6.

2. DESCRIPTION OF THE PECAP ALGORITHM

The PECAP algorithm attempts to estimate AP from matrix $\boldsymbol{M}$. A synopsis of the main steps followed by the algorithm and the necessary assumptions are reported in this section. The reader is referred to [5] for a mathematical formulation.

2.1. Assumptions

2.1.1. Symmetry of the matrix $\boldsymbol{M}$

This is equivalent to state that $M_{p,m} = M_{m,p}$ for any probe electrode p and masker electrode m. For a given set of electrodes N, the dimensionality of the matrix $\boldsymbol{M}$ is $[N \times N]$.

2.1.2. Gaussian activation patterns

The AP for each electrode is Gaussian, and is therefore described by mean (μ), width (σ) and amplitude. Hence, in order to reconstruct the APs for a set of electrodes N, we need to compute the parameter matrix $\boldsymbol{B}$ of dimensionality $[N \times 3]$.

2.1.3. Equal-area activation patterns

As all electrodes are stimulated to produce the same loudness, it is assumed that their APs have the same area. This assumption allows a simplification of the amplitude Gaussian parameters in $\boldsymbol{B}$ that needs to be estimated, thus reducing its dimensionality to $[N \times 2]$.

2.2. Algorithm Workflow

The algorithm includes a number of steps and two nonlinear optimization stages. In the first step, the matrix $\boldsymbol{M}$ estimated from the ECAP amplitudes is linearly normalized so that all ranges of values are within 1 and 0. This normalization approach has been revised, as described in more detail in the next subsection. The normalized matrix $\boldsymbol{M}$ is then averaged across its diagonal to reduce measurement noise (under the symmetry assumption in *2.1.1*). The output is processed through STAGE I and STAGE II of the algorithm, which determine numerically the parameters μ and σ for each electrode that minimize the error between measured and reconstructed $\boldsymbol{M}$. The optimization algorithm is based on the Barrier method [10] and uses constraints different for STAGE I and II.

STAGE I finds a solution $\boldsymbol{A}$ of Eq. 2 where means and widths are within range of "physiologically normal" activation patterns. This is obtained by imposing the following constraints: means of the AP for any probe electrode p were within one electrode of the stimulating electrode (i.e., $p - 0.5 < \mu_p < p + 0.5$); the standard deviations of the AP for all electrodes were smaller than 6 electrodes.

STAGE II was designed to detect *unwanted exceptions* as described in the Introduction. The constraints on the Gaussian APs were relaxed in one of two ways: (1) "Shifted Peak" (SP), allowing the mean of the activation to be away from the stimulating electrode; (2) "Bimodality" (BI), allowing single instances of bimodal excitation patterns. These two steps are run in parallel and allow the constraints to be relaxed on only one electrode at a time. The fitting residual between the original and the reconstructed $\boldsymbol{M}$ after STAGE I is compared to that after each iteration of STAGE II; if the latter reduces the error by at least 10%, the PECAP has predicted an instance of bimodality of shifted peak.

3. MODIFICATION TO THE PECAP

The estimation of the mean and width parameters in $\boldsymbol{B}$ of STAGE I and II may depend on the range of amplitudes in the ECAP matrix $\boldsymbol{M}$. Since the amplitudes of the Gaussian AP for all electrodes are independently adjusted to maintain the equal area constraint (see *2.2.3*), the optimization may converge to inaccurate solution to minimize the residual between measured and modelled $\boldsymbol{M}$. We revised this stage by adding a linear normalization step for all channels in the range $(0, \sqrt{2\pi}\sigma_0]$, with $\sigma_0 = 3$ chosen as the median of the width values allowed by the PECAP (0 to 6]. Additionally, we introduced area normalization in the modelling of the AP using a scaling factor $G\sqrt{2\pi}\sigma$, where G is the peak amplitude of the Gaussians at each iteration. This allows a more careful estimation of the area around the edges of the array as it does not depend on the number of available samples (i.e., the number of masker electrodes). Altogether, these modifications are used to reinforce the assumptions made in 2.1.

4. EXPERIMENTAL SETUP

4.1. Physiological data

The revised PECAP algorithm was run on the ECAP measurements from nine adult users of HiRes90k Advanced Bionics® cochlear implants [6]. Subject details are reported in Table 1. A forward-masking procedure described in [8] was employed. According to this procedure, ECAP for a combination of a probe electrode and a masker electrode are obtained by subtracting the responses from four stimuli: (A) probe alone (B), masker + probe, (C) masker alone, and (D) baseline activity. It has been shown that the stimulation artifact - which can be several orders of magnitude larger than the neural response - is vastly attenuated by subtracting the four responses as: $A - (B - C) - D$ [8, 11, 12]. The Bionic Ear Data Collection System (BEDCS) version 1.18.315 (Advanced Bionics, Valencia, CA) was used to produce the electrical stimulation and record all responses. The gain of the amplifier in the BEDCS was set to 300 and the sampling rate to 56 kHz. Stimuli were monopolar biphasic pulses (32 μs per phase) delivered at 20-pps rate. The level of the pulses was adjusted to elicit the same loudness across all electrodes. This was determined behaviorally for each electrode by increasing the level on the Advanced Bionics clinical loudness chart, and noting the

loudness reports from the subjects. The current level which corresponded to "most comfortable listening level" (MCL, point 8 in the chart) was chosen as stimulating level for all electrodes to obtain ECAP measurements. An additional loudness balancing was performed at MCL by presenting the stimulus consecutively across four electrodes; if electrodes differed in loudness, these were adjusted in level and their relative loudness was estimated again.

To measure the ECAP masking pattern for any probe electrode p, the location of the probe stimulus was fixed whilst the electrode location of the masker stimulus was varied. Hence, for a number of electrodes N, there were N^2 combinations, where $N = 16$ for all subjects except S5 ($N = 15$).

4.2. Data extraction

The ECAP measure for each condition was an average of 100 sweeps. Extraction of the ECAP amplitudes (used to populate the $\boldsymbol{M}$ matrix) was performed off-line using MATLAB® software. The waveforms were first inspected visually to exclude outliers and set two waveform markers: the first negative peak ($N1$; occurring at approximately 240 μs) and the subsequent positive peak ($P1$; occurring at 440 μs). The ECAP amplitude was computed as $P1 - N1$. Waveforms with amplitudes smaller than 30 μV were labelled as "no response" and set to zero.

ID	Ear	Age	Age at Hearing Loss	Age at Surgery	Possible Etiology	Array/Spacing (mm)
S1	R	74	55	66	Genetic	HiFocus Helix/0.85
S2	L	84	47	77	Noise	HiFocus 1J/ 1.1
S3	L	50	17-18	46	Otosclerosis	HiFocus 1J/ 1.2
S4	L	52	3	50	EVA	HiFocus 1J/ 1.3
S5	L	49	0 (R), 42 (L)	43	Rubella	HiFocus 1J/ 1.4
S6	R	64	50	50	Unknown	HiFocus 1J Posit. / 1.1
S7	R	68	50	67	Noise	Mid-Scala/ 0.85
S8	R	67	14	66	Unknown	HiFocus 1J/ 1.2
S9	R	38	28	37	Unknown	Mid-Scala/ 0.85

Table 1. Subjects' details at the time of testing.

5. RESULTS and DISCUSSION

5.1. Detection of exceptions

The PECAP algorithm was run on the ECAP matrix ($\boldsymbol{M}$) as measured for the nine subjects in Table 1. The values of the means and widths of the Gaussian APs as predicted by the PECAP algorithm are shown in Figure 1. One instance of shifted peak was detected for subject S6 on E9. Here, a better fit was obtained after STAGE II by modelling the AP for E9 as a Gaussian centered on electrode 10.5. For the other subjects, visual inspection of Figure 1 reveals patterns that are consistent with regions of lower neural density. For instance, near E3 and E12 in S8, the activation patterns of both basal and apical electrodes peak further away from their geometric mean, consistent with an instance of limited neural survival in that area. Conversely, no instances of cross-turn stimulation were detected. In a previous report ([5]) we found evidence of exceptions in two out of five subjects. The result from the present study is, however, in line with the overall good speech performance of the subjects.

The widths were variable from subject to subject, and from electrode to electrode ($\langle 1.8 \rangle \pm 0.6$) as shown by shades of grey in Figure 1.

Figure 2 shows the measured and reconstructed ECAP amplitudes ($\widehat{\boldsymbol{M}}$, $\boldsymbol{M}_{\boldsymbol{STAGE\ I}}$ and $\boldsymbol{M}_{\boldsymbol{STAGE\ II}}$, in the top subplot), and the neural activation patterns after STAGE I and II (bottom subplot) estimated by PECAP for subject S6, which data had shown a shifted peak on E9. It can be noted that the AP after STAGE II (shown in blue) significantly improves the fit with the observed $\widehat{\boldsymbol{M}}$ (in grey) relative to the fit obtained after STAGE II (in red).

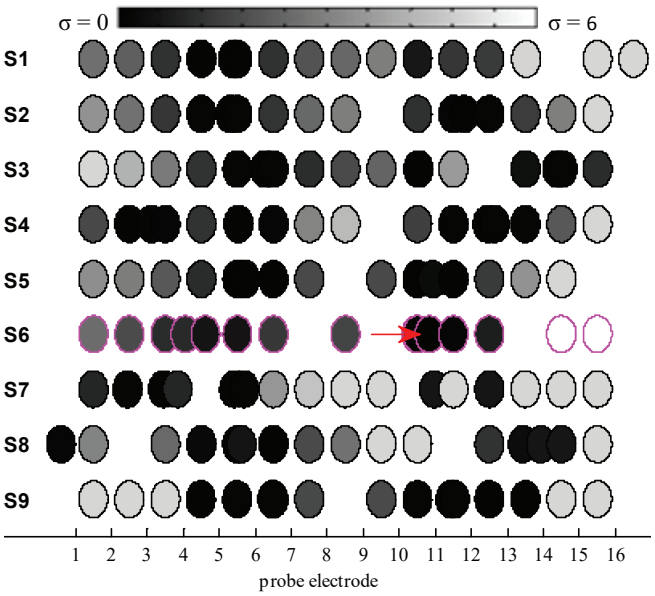

Figure 1. Graphical representation of the final means (center of each circle) and widths (grayscale) as estimated by the PECAP as function of probe electrode for all nine subjects. The red arrow indicates the instance of shifted peak detected for subject S6 on E9.

5.2. SNR estimation in the ECAP data

Given the clinical application of the PECAP algorithm as diagnostic tool to detect poor-performing channels, it is important to estimate the reliability of its prediction as

function of the noise in the measurement. We measured the signal-to-noise ratio (SNR) in the physiological data as the power ratio between the initial segment of the ECAP waveform – mostly dominated by the neural response – and the final segment of the waveform – mostly dominated by noise. The results were as follows [dB]: 4.9 (S1), 5.1 (S2), 3.0 (S3), 1.4 (S4), 3.9 (S5), 4.2 (S6), 1.4 (S7), 1.7 (S8), 1.6 (S9). While this is a relative measure, a particularly low SNR should be taken as indication of unreliable ECAP data, and, as such, any prediction made by the PECAP that relies on such data might carry the same limited reliability. Note that these SNRs were derived using a different method than in [5], and so are not directly comparable.

5.3. On the importance of the PECAP analysis

Solving the inverse problem in Eq. 2 is necessary to recover reliable information about the electrode-to-neuron interface for every channel. Simple measurements of ECAP patterns may not reveal this information. This is because the excitation patterns of both masker and probe influence the measured response. Figure 3 reports an instance of ECAP data that could lead to inaccurate conclusions on the underlying neural activation pattern. The measured ECAP response for S1 on E2 (in grey) shows an instance of shifted peak (in E3) and possibly a bimodality, with a second peak on E5. Conversely, the AP for the same channel reconstructed by the PECAP (in red) is described by a unimodal distribution. After analyzing $\mathbf{A}_{\text{STAGE I}}$, the measured ECAP pattern could be explained as combination of the APs from all other electrodes. Note that the ECAP reconstructed from $\mathbf{A}_{\text{STAGE I}}$ (i.e, $\mathbf{M}_{\text{STAGE II}}$ in blue) can approximate quite closely the measured patterns. CT scan for S1 also did not reveal plausible basis for bimodality.

6. CONCLUSION

We described an approach to recover neural activation patterns from physiological data in cochlear implant subjects. The main clinical use of this approach – that we termed PECAP – is to detect poor-functioning channels. The PECAP was applied to data measured from nine cochlear implant users, revealing clinically useful information, such as possible instances of "dead regions". At present, the method is limited in the number of exceptions it can to identify (one per channel), and in the robustness to parameterizations of the algorithm. We are currently addressing these limitations, with the intention of developing PECAP to the stage where it can be implemented in a clinical environment to inform patient-specific stimulation strategies.

7. ACKNOWLEDGMENTS

This work was supported by the MRC (MC-A060-5PQ70) and by Action on Hearing Loss (MC-A060-5PQ75).

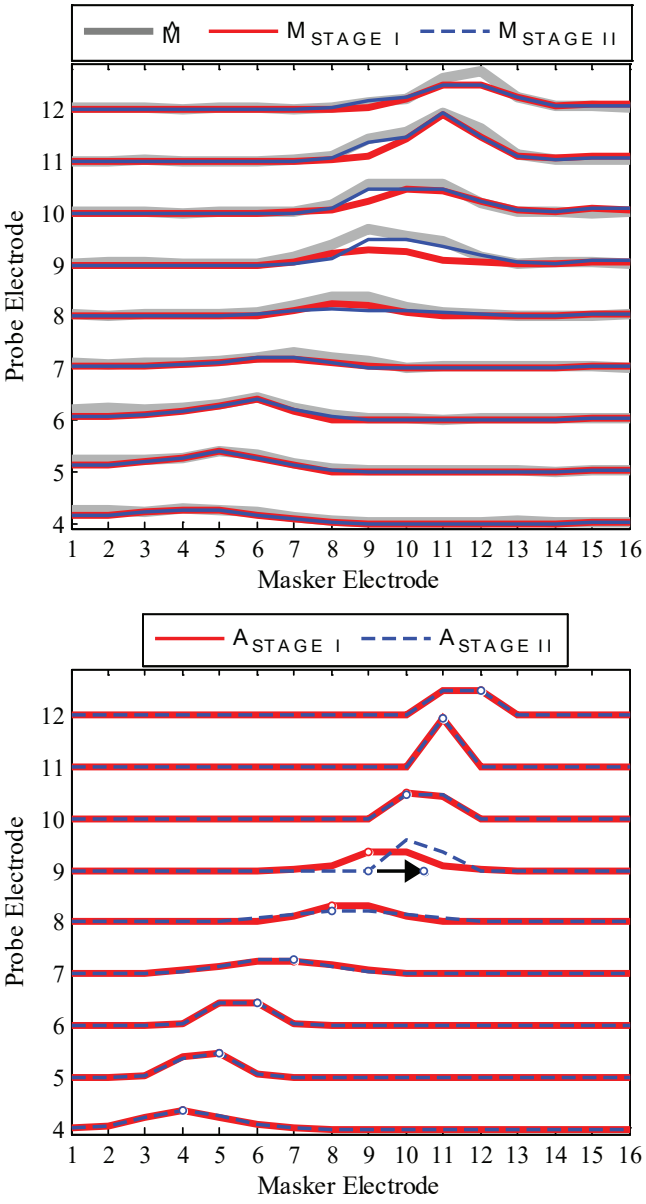

Figure 2. Measured and modelled ECAP patterns (top) and activation patterns (bottom) after STAGE I (red) and STAGE II (blue) for S6. Only channels 4 to 12 are shown in the ordinates to improve readability of the figure.

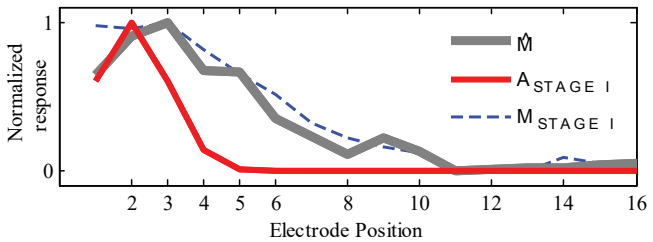

Figure 3. Normalized ECAP (i.e., $\boldsymbol{M}_{9,k}$) and AP (i.e., $\boldsymbol{A}_{9,k}$) for subject S1 on electrode E2.

9. REFERENCES

[1] B. S. Wilson and M. Dorman, "Cochlear implants: Current Designs and Future Possibilities," *Journal of rehabilitation research and development,* vol. 45, pp. 695-730, 2008.

[2] L. K. Holden*, et al.*, "Factors affecting open-set word recognition in adults with cochlear implants," *Ear and hearing,* vol. 34, pp. 342-360, 2013.

[3] J. A. Bierer*, et al.*, "Identifying cochlear implant channels with poor electrode-neuron interface: electrically-evoked auditory brainstem responses measured with the partial tripolar configuration," *Ear & Hearing July/August,* vol. 32, pp. 436-444, 2011.

[4] J. H. Noble*, et al.*, "Clinical Evaluation of an Image-Guided Cochlear Implant Programming Strategy," *Audiology and Neurotology,* vol. 19, pp. 400-411, 2014.

[5] S. Cosentino*, et al.*, "Multistage nonlinear optimization to recover neural activation patterns from evoked compound action potentials of cochlear implant users," *Biomedical Engineering, IEEE Transactions on,* vol. PP, pp. 1-1, 2015.

[6] L. A. DeVries*, et al.*, "The electrically evoked compound action potential, computerized Tomography, and behavioral measures to assess the electrode-neuron Interface," in *Conference on Implantable Auditory Prostheses*, Lake Tahoe, California, 2015, p. 219.

[7] C. J. Brown*, et al.*, "Electrically evoked whole-nerve action potentials: Data from human cochlear implant users," *The Journal of the Acoustical Society of America,* vol. 88, pp. 1385-1391, 1990.

[8] L. T. Cohen*, et al.*, "Spatial spread of neural excitation in cochlear implant recipients: comparison of improved ECAP method and psychophysical forward masking," *Hearing Research,* vol. 179, pp. 72-87, 2003.

[9] B. C. J. Moore and J. I. Alcantara, "The Use of Psychophysical Tuning Curves to Explore Dead Regions in the Cochlea," *Ear & Hearing,* vol. 22, pp. 268-278, 2001.

[10] R. H. Byrd*, et al.*, "A trust region method based on interior point techniques for nonlinear programming," *Mathematical Programming,* vol. 89, pp. 149-185, 2000/11/01 2000.

[11] L. T. Cohen, "Practical model description of peripheral neural excitation in cochlear implant recipients: 3. ECAP during bursts and loudness as function of burst duration," *Hearing Research,* vol. 247, pp. 112-121, 2009.

[12] P. J. Abbas*, et al.*, "Channel Interaction in Cochlear Implant Users Evaluated Using the Electrically Evoked Compound Action Potential," *Audiology and Neurotology,* vol. 9, pp. 203-213, 2004.